

Numerical Solutions of Nano/Microphenomena Coupled With Macroscopic Process of Heat Transfer and Fluid Flow: A Brief Review

Ya-Ling He

Key Laboratory of Thermo-Fluid Science and Engineering of MOE,
School of Energy and Power Engineering,
Xi'an Jiaotong University,
Shaanxi 710049, China

Wen-Quan Tao¹

Key Laboratory of Thermo-Fluid Science and Engineering of MOE,
School of Energy and Power Engineering,
Xi'an Jiaotong University,
Shaanxi 710049, China
e-mail: wqtao@mail.xjtu.edu.cn

In this paper, numerical simulation approaches for multiscale process of heat transfer and fluid flow are briefly reviewed, and the existing coupling algorithms are summarized. These molecular dynamics simulation (MDS)–finite volume method (FVM), MD–lattice Boltzmann method (LBM), and direct simulation of Monte Carlo method (DSMC)–FVM. The available reconstruction operators for LBM–FVM coupling are introduced. Four multiscale examples for fluid flow and heat transfer are presented by using these coupled methods. It is shown that by coupled method different resolution requirements in the computational domain can be satisfied successfully while computational time can be significantly saved. Further research needs for the study of multiscale heat transfer and fluid flow problems are proposed. [DOI: 10.1115/1.4030239]

Keywords: numerical simulation, multiscale system, multiscale process, coupled method, reconstruction operator, heat transfer and fluid flow

1 Introduction to Multiscale Simulation

In both engineering and nature, system or process often covers several geometric or time scales. Physical process in such system/process is called multiscale problem. Actually almost all problems have multiple scales in nature. Because of the limitations in the development of science and technology, previous studies were mainly concentrated at individual scale level. With the rapid development of computer hardware and numerical methods, multiscale simulation has now become a hot topic in both thermal science and engineering [1]. In this paper some recent numerical practices, basically of the authors' group, in simulating multiscale heat/mass transfer and fluid flow problems will be reviewed and briefly presented. It should be noted that the characteristic value in space is closely related to the characteristic value in time. In the following presentation, focus will be mainly put on the space aspect, and when needed the related time scale will also be described.

1.1 Two Typical Examples of Multiscale Heat/Mass Transfer Problems

Example 1: Transport process in proton exchange membrane fuel cell (PEMFC).

A schematic view of a PEMFC is shown in Fig. 1. It can be seen that the transport and reaction processes in a PEMFC are very complicated and the dimensions of different components are very different with a variation covering 3–4 orders.

In the present-day numerical simulation of PEMFC usually FVM is adopted, and a number of empirical parameters are involved with their values being selected with great uncertainty. The polarized (V – I) curve is usually taken to verify a simulation model. As many as 13 empirical parameters may be involved in simulations [2–9]. The values of each parameter span quite a wide range. In addition, different parameter may have qualitatively

different effect on the V – I curve. This leads to following unpleasant situation: With two different sets of empirical parameters, we may obtain almost the same output curve [10,11]. Only multiscale simulation can avoid such an unpleasant situation, which will be explained in the later presentation.

Example 2: Cooling of electronic devices in a data center.

The cooling stream in a data center or a large room for supercomputer experiences several orders of geometric variation: from a cabinet with dimension of meters to a chip with dimension of several centimeters (Fig. 2). The fluid flow and heat transfer processes at different scale levels are all governed by the N–S equations and energy equation. When doing numerical simulation for the cooling process how to master the characteristics of the whole process while do not neglecting the details of some important components or elements (such as chips) is a very challenging task.

1.2 Two Categories of Multiscale Problems. After working on a number of different kinds of multiscale problems, we have found that from a numerical simulation perspective the multiscale problems in thermofluid science and engineering may be divided into following two categories [1,12].

1.2.1 Multiscale System. For a multiscale system, the phenomena at different scales are governed by the same governing equations and can be solved by the same numerical method. Cooling simulation in the data center is a typical multiscale system problem. Nie and Joshi [13] proposed a top-to-down sequential simulation method with increasing fineness of grid to solve a multiscale system. The major idea of their method is as follows. First, system level analysis is performed with simplified models on a relatively coarse grid; next, local convective heat transfer coefficients, and so on are extracted from the previous simulation results, and used as the boundary conditions for a next level simulation; such simulation is continued until to the lowest level. The key of such a top-to-down sequential simulation method is how to simplify the entire system with not-too-fine grid, while still obtaining accurate enough results, from which the boundary

¹Corresponding author.

Manuscript received May 4, 2014; final manuscript received September 11, 2014; published online May 14, 2015. Assoc. Editor: Yogesh Jaluria.

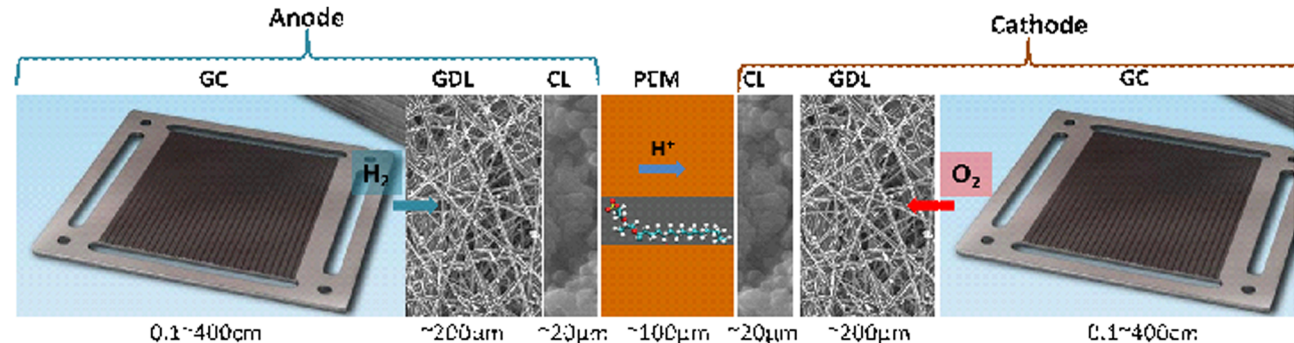


Fig. 1 A schematic diagram of PEMFC

conditions are extracted for the next level simulation. For cooling of electronic devices, the thermal resistance analysis method was proposed by the authors' group for this purpose. The focus of the present paper is on the numerical solution of multiscale process, so the details of the thermal resistance analysis method are not presented here. Interested readers may consult Refs. [14] and [15].

1.2.2 Multiscale Process. For a multiscale process, phenomena at different scales are governed by different equations and solved by different numerical methods. Process in a PEMFC is a typical multiscale process. For the multiscale simulation of a PEMFC, numerical approaches at different geometric scales are adopted. FVM for macroscopic process, LBM/DSMC for mesoscopic process, and molecular dynamic simulation (MDS) for microscopic process, are adopted for different subregions with different geometric scales. The three-scale numerical approaches may be adopted individually or coupled.

- (1) Individual adoption: methods of atomic scale, nano/microscale are adopted to determine process parameters or source terms, which are used for the upper scale simulation [16–18].
- (2) Coupled adoption: methods of nanoscale, microscale, and macroscale are adopted for different regions of the problem studied, and solutions are exchanged at the interfaces to obtain the entire full solution. In some sense this method is more challenging in that the physical processes at different geometric scales are coupled in reality and should be expressed in numerical aspect. Such numerical method can be described as "Solving regionally and coupling at interface." The most challenging aspect is the numerical solutions (information) exchange at the interfaces of the neighboring regions, which can be mathematically expressed as [1,12]

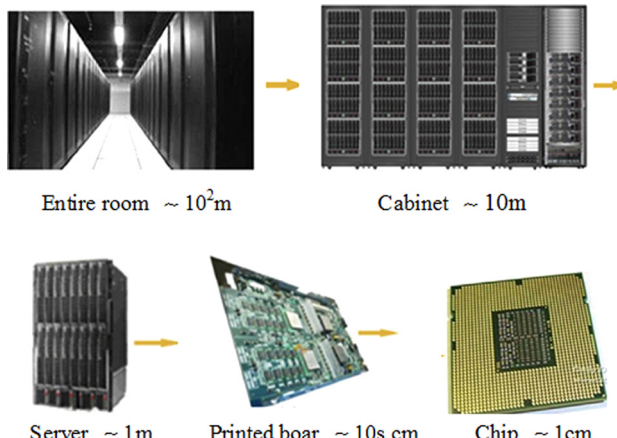


Fig. 2 Different facilities encountered by cooling stream in a data center

$$\Phi = \mathbf{C}\phi \quad (1a)$$

$$\phi = \mathbf{R}\Phi \quad (1b)$$

where Φ and ϕ are the macroscopic and microscopic variables, respectively; \mathbf{C} and \mathbf{R} are compression and reconstruction operators, respectively. The compression operator \mathbf{C} compresses a larger number of information obtained in the numerical solution of micro- or nanoscale level, and is easy to be found such as different averaging methods, while the reconstruction \mathbf{R} is difficult to be constructed (developed). Such operators should be physically meaningful, mathematically stable, computationally efficient, and easy to be implemented.

It is worth noting here that by the terminology "operator" we mean

- (1) it is an actual mathematical formula.
- (2) it is a set of numerical treatments for transferring information (composite reconstruction operator).

At this point, we may briefly summarize the numerical approaches for multiscale problems as shown in Fig. 3.

As indicated above for the coupled methods the key is to find the reconstruction operator. In the following, some recent results of this operator are presented. Their application examples will be presented later.

2 Coupling Methods and Some Reconstruction Operators

As indicated above in the coupled method solutions from neighboring regions have to be exchanged at their interface in order to maintain the solution consistency for the entire domain. The information exchange process at the interface and the reconstruction operators developed so far are presented in this section.

2.1 Brief Description of Coupled Solution Method. Usually the domain is divided into three regions: continuum region (CR),

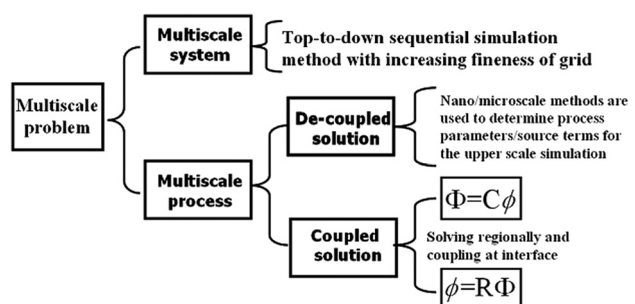


Fig. 3 Numerical approaches for multiscale heat transfer and fluid flow problems

particle region (PR), and hybrid region (HR). Exchange of information is conducted at the two interfaces. The basic consideration for information exchange is to satisfy some conservation conditions and the consistency of dependent variables solved from different approaches. Such information exchange in the HR should be conducted repeatedly until convergence is reached. Such coupling was first given by O'Connel and Thompson in 1995 for MDS with finite difference method (FDM) [19].

Taking the coupling of FVM with LBM (CFVLLBM) as an example, the coupling procedure is as follows:

Step 1: With an assumed initial boundary conditions at the interface, the FVM simulation is performed.

Step 2: After a temporary solution is obtained, the information at the line within HR is transformed using the proposed reconstruction operator.

Step 3: The LBM simulation is carried out in the LBM zone.

Step 4: The temporary solution of LBM at the line within HR is transported into the macrovariables and the FVM simulation is repeated.

Step 5: Such computation is repeated until the results in the computational domain reach convergence standard.

2.2 Reconstruction Operators. Numerical data obtained in the solutions of micro- or nanoscale level are much larger than that included in the macroscale solution. Thus the transfer of solution with less data to that with more data, i.e., the reconstruction of solution with more data from solution with less data is the key of such coupling. In the following presentation existing reconstruction operators are introduced for different coupled pairs: LBM with FVM, MDS with FVM, MDS with LBM, and DSMC with FVM.

2.2.1 Coupling of LBM With FVM (FDM/Finite Element Method (FEM))

(1) Velocity component

By the multiscale expansion technique and assuming velocity field is free from source, it can be obtained [20]

$$\begin{aligned} f_i &= f_i^{(0)} + \varepsilon f_i^{(1)} + \varepsilon^2 f_i^{(2)} + \dots \\ &= f_i^{(\text{eq})} \left[1 - \tau \Delta t U_{i\beta} c_s^{-2} \left(U_{i\alpha} \partial_{x_\alpha} u_\beta + \nu \partial_{x_\alpha}^2 u_\beta + \nu \rho^{-1} S_{\alpha\beta} \partial_{x_\alpha} \rho \right) \right] \end{aligned} \quad (2)$$

where $f_i^{(0)}$, $f_i^{(1)}$, and $f_i^{(2)}$ are the zero, first, and second order expressions of the distribution function. ε is the small expansion parameter, which can be viewed as the Knudsen number Kn (the ratio of the mean free path over the characteristic length scale of the flow).

In the above equation, the left hand side is the LBM distribution function of velocity component; while the right hand side represents the variables of FVM and known lattice parameters. Other parameters in Eq. (2) are explained as follows:

$$S_{\alpha\beta} = \partial_{x_\beta} u_\alpha + \partial_{x_\alpha} u_\beta$$

$$U_{i\alpha} = c_{i\alpha} - u_\alpha$$

where α is the coordinate direction, ∂_{x_α} is the space derivative with respect to α direction, $c_{i\alpha}$ is the α -component of lattice velocity c_i , u_α is the α -component of physical velocity u , and τ is the relaxation factor for the density function of velocity component.

(2) Temperature

If the LBM for thermal flows adopts the double distribution function model, then the reconstruction operator for distribution function of temperature is as follows [21]:

$$\begin{aligned} g_i &= g_i^{(\text{eq})} \left\{ 1 - \tau_g \Delta t T^{-1} \left[U_{i\alpha} \partial_{x_\alpha} T + a_T (\partial_{x_\alpha})^2 T \right] \right\} \\ &\quad + \frac{\tau_g \omega_i T c_{i\beta}}{\tau_f U_{i\beta}} \frac{(f_i - f_i^{(\text{eq})})}{f_i^{(\text{eq})}} + \tau_g \Delta t \omega_i c_{i\beta} T \rho^{-1} \partial_{x_\beta} \rho \end{aligned} \quad (3)$$

where g_i is the density distribution function for temperature and T is the thermodynamic temperature.

(3) Concentration

For mass transport process, adopts the double distribution function model. The reconstruction operator for the density function of component concentration is [22]

$$\begin{aligned} g_i &= g_i^{(\text{eq})} [1 - \tau_g \Delta t Y^{-1} (U_{i\alpha} \partial_{x_\alpha}^{(1)} Y - D \partial_{xx} \partial_{x_\alpha} Y)] \\ &\quad - 0.5 \tau_g \Delta t Y c_{i\beta} (U_{i\alpha} \partial_{x_\alpha}^{(1)} u_\beta + \nu \partial_{x_\alpha} \partial_{x_\alpha} u_\beta \\ &\quad + \rho^{-1} \nu S_{\alpha\beta} \partial_{x_\alpha} \rho) + 0.5 \tau_g \Delta t \rho^{-1} Y c_{i\beta} c_s^{-2} \partial_{x_\beta}^{(1)} \end{aligned} \quad (4)$$

where Y is the macroconcentration component and g_i is the distribution function.

(4) General reconstruction operator for scalar variables

In energy and environmental engineering many dependent scalar variables obey following convection-diffusion equation:

$$\frac{\partial \phi}{\partial t} + \mathbf{u} \cdot \nabla \phi = \Gamma \Delta \phi + S \quad (5)$$

It can be shown that the reconstruction operator for component concentration presented above actually is the generalized reconstruction operator for all scalar variables governed by Eq. (5), with individual relative lattice parameters (equilibrium distribution function and relaxation factor) [23].

2.2.2 Coupling of MDS With FVM (FDM/FEM)

(1) Space coupling between MDS–FVM

A schematic picture of the overlapped region is presented in Fig. 4(a). In the bulk region over the upper dashed line interface the continuum method (FVM) is used; in the region below the lower interface (dashed line) the microscopic method (MDS) is adopted, and an overlap region exists in between, where both methods are valid and used, and information exchange is finished therein.

For the information exchange, three layers shown in Fig. 4(b) are dealt with as follows:

In the P–C layer: the macroscopic quantities averaged from PR (MDS) are given to FVM as boundary conditions

Buffer layer: kept to reduce the effect of artificial intervention

In the C–P layer: the information from FVM is transferred to all the particles in this layer whose velocities or accelerations are changed accordingly

(2) Time step coupling between MDS–FVM

As indicated in Sec. 1 the time steps of MDS and FVM are quite different. The time instant match of the two solutions should also be guaranteed. The ratio of time steps $\delta t^C / \delta t^P$ is case dependent and should be determined by trial and error for individual problem. Its value is usually in the order of hundreds. The time step of FVM should be small enough in order to ensure numerical accuracy, and it should satisfy the principle that it is much smaller than the characteristic times for velocity and temperature [24]. In addition, too large δt^C will also weaken the coupling. On the other hand, it should be large enough for MD to provide available information in a single step of δt^C , especially for gas. Once the ratio is determined, the transfer of information may be conducted as shown in Fig. 5 [25]. As shown there, the averaged value from

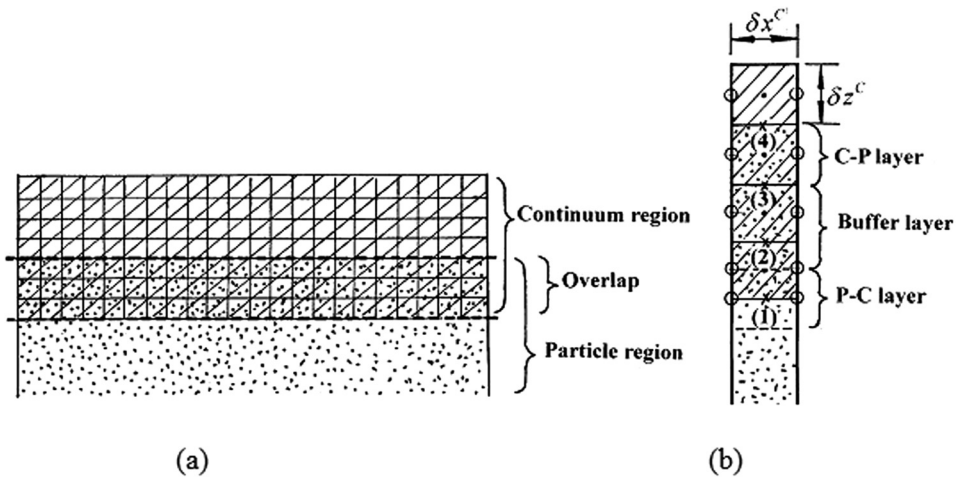


Fig. 4 Space coupling between MDS and FVM. (a) Three regions and (b) interface coupling.

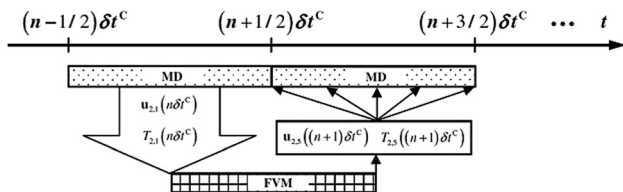


Fig. 5 Time step coupling between MDS and FVM [25]

MDS is transferred to FVM, then one time step of δt^C forward is conducted in FVM, and the solution of FVM is retransferred to all the tiny time steps for MDS within 1 step of δt^C . Such alternative transferring is repeated until the instant required or converged solution is reached.

(3) Momentum coupling between MDS–FVM (C–P layer)

For the C–P layer, the mass and momentum consistence requires the synchronization between the averaged molecular velocity and the macroscopic velocity. For this purpose, the acceleration of each molecule in C–P layer should be modified as shown in Fig. 6. The accelerations of particles are revised at every time step in order that the averaged velocity of particles in C–P layer may be equal to the target velocity.

(4) Energy coupling between MDS–FVM (C–P layer)

The thermal coupling is also realized through Langevin method as shown in Fig. 7 [26]. The temperature of solid wall or some part of the system can be kept constant with the aid of the damping force and the random force presented below.

$$\ddot{\mathbf{r}}_i(t) = -\alpha_1 \dot{\mathbf{r}}_i(t) + \frac{\mathbf{f}_i(t)}{m} + \frac{\mathbf{F}(t)}{m}$$

Damping force

Random force related to the target temperature

Fig. 7 Thermal energy coupling for molecules in C–P layer

(5) Boundary force model for MDS–FVM coupling

In the conventional MDS the periodic boundary condition is used based on the assumption of an infinite space. However, in the MD–continuum multiscale simulations, MDS can only be used in part of the entire domain, so the boundary force acted on particles near the boundary from imaginary particles outside should be considered (Fig. 8). The implementation of nonperiodic boundary condition, which is often used in multiscale atomistic–continuum simulations has been investigated by the authors' group. Based on simulation results of the relationship between the boundary force and different fluid states (different temperatures and densities) at the boundary, fitting formulas of the boundary force are proposed. The accuracy of fitting formulas is verified through the comparison with the equilibrium MDS results [27].

$$\ddot{\mathbf{r}}_i(t) = \frac{1}{(p/2+1)\delta t^p} \left[\mathbf{u}(t+\delta t^p) - \left\langle \frac{1}{N^{C-P}} \sum_{j=1}^{N^{C-P}} \dot{\mathbf{r}}_j(t) \right\rangle_{p\delta t^p} \right] + \left[\frac{\mathbf{f}_i(t)}{m} - \left\langle \frac{1}{N^{C-P}} \sum_{j=1}^{N^{C-P}} \frac{\mathbf{f}_j(t)}{m} \right\rangle_{p\delta t^p} \right]$$

Revised acceleration of particle *i*

Target velocity

Averaged velocity in C–P layer

Force on particle *i* from other particles

Averaged force in C–P layer

Fig. 6 Momentum coupling for molecules in C–P layer

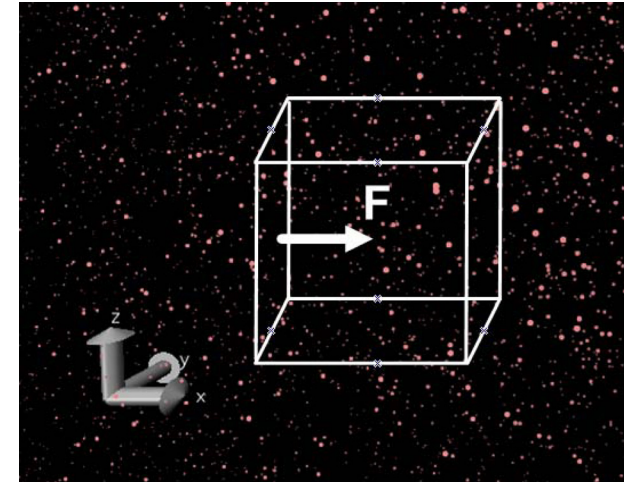


Fig. 8 Boundary force for limited space of MD simulation

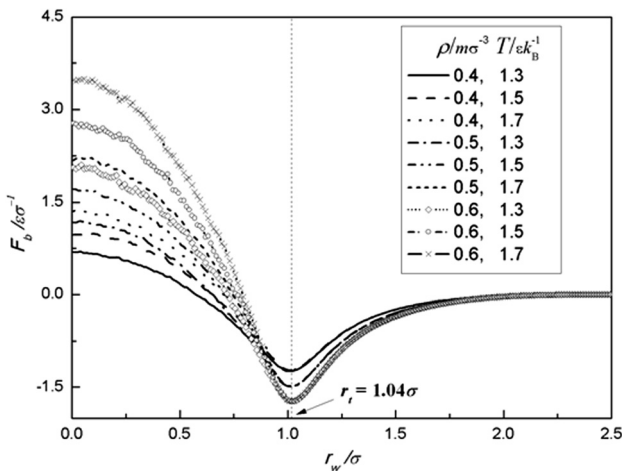


Fig. 9 Boundary force variation with fluid state

Our results of the boundary force mentioned above are presented in Fig. 9. As can be seen there, the boundary force can be divided into two parts: the left part is a function of density and temperature, while the right part is a function of density only.

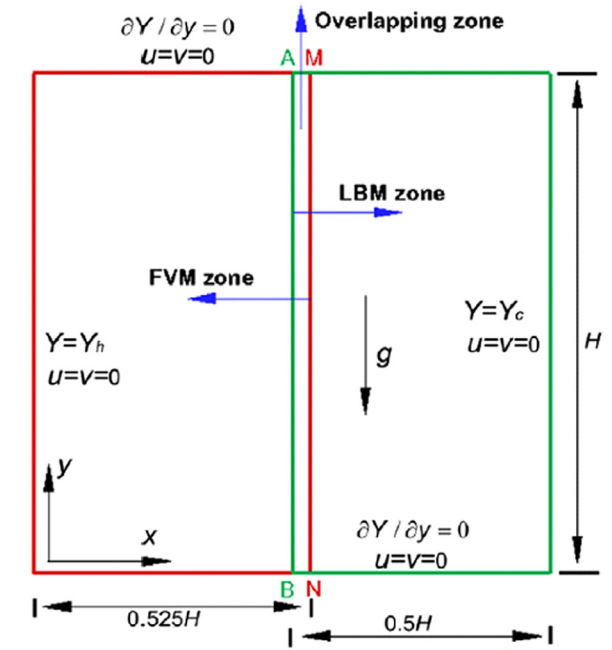


Fig. 11 Natural convection in a square cavity caused by concentration gradient [23]

Based on the data at 84 different state points, following fitted formulas can be used to describe the boundary force:

$$F_b = \begin{cases} p_1 + p_2 e^{(r_w+0.25)^{3.4}} \cos(p_3 r_w) & \text{for } r_w \leq 1.04 \sigma \\ \frac{-1}{q_1 + q_2 (2.5 - r_w)^2 + \frac{q_3}{(2.5 - r_w)^2}} & \text{otherwise,} \end{cases} \quad (6)$$

where r_w is the distance between the atom and the boundary, and p_1, p_2, p_3, q_1, q_2 , and q_3 are six parameters, among which the three former ones are functions of density and temperature and the three latter ones are functions of density only. The expressions of the parameters are as follows:

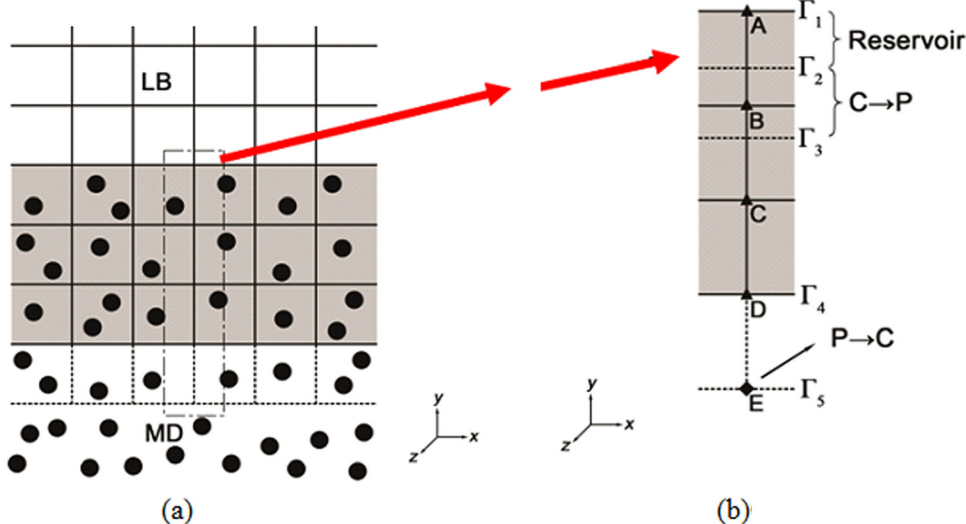


Fig. 10 Space coupling between MDS and LBM [30]. (a) Three regions and (b) coupling details.

$$p_1 = \frac{(-18.953 + 53.369T - 1.253T^2 + 4.599T^3 + 59.871\ln(\rho) + 19.737(\ln(\rho))^2)}{(1 + 2.592T - 0.557T^2 + 0.049T^3 - 13.912\ln(\rho) + 18.657(\ln(\rho))^2)} \quad (7)$$

$$p_2 = \frac{(-0.094 + 2.808T - 0.019T^2 - 0.001T^3 + 2.823\ln(\rho) + 2.071(\ln(\rho))^2)}{(1 + 0.168T - 0.013T^2 - 4.323\ln(\rho) + 2.557(\ln(\rho))^2 - 2.155(\ln(\rho))^3)} \quad (8)$$

$$p_3 = 3.934 + 0.099T^{0.394} - 0.097\rho^{17.437} + 0.075T^{0.394}\rho^{17.437} \quad (9)$$

$$q_1 = -30.471 + 113.879\rho - 207.205\rho^2 + 184.242\rho^3 - 62.879\rho^4 \quad (10)$$

$$q_2 = 6.938 - 25.788\rho + 46.773\rho^2 - 41.768\rho^3 + 14.394\rho^4 \quad (11)$$

$$q_3 = 39.634 - 147.821\rho + 269.519\rho^2 - 239.066\rho^3 + 81.439\rho^4 \quad (12)$$

In the simulations for obtaining numerical data shown in Fig. 9, the boundary force is a function of density and temperature, so Eq. (6) can be used in the fluid flow and heat transfer problems with changing density and temperature, such as Poiseuille flow problems with viscous dissipation and unsteady heat transfer problems. This boundary force model can also be used in multi-scale MDS–continuum method or full MD simulation with complicated boundaries. The main limitation of this model is that it can only be used for Lennard–Jones potential and dense fluid.

2.2.3 Coupling of MDS With LBM. As shown in Fig. 10, for the coupling of MDS with LBM, three regions are set up with a HR in between where both MD and LBM simulations are conducted. The details of space coupling are as follows:

C–P layer: The velocities of particles in this layer are reset through a Maxwellian distribution with mean and variance consistent with the macroscopic velocity and temperature from LBM:

$$P(\mathbf{u}_i) \propto \exp[-m(\mathbf{u}_i - \mathbf{u})^2/(2k_B T)] \quad (13)$$

P–C boundary: The distribution function of LBM is reconstructed from the information of MDS, and the reconstruction operator shown by Eq. (2) is adopted.

2.2.4 Coupling DSMC With FVM (Solid). For rarefied gas flow in a micronozzle and the nozzle wall temperature simulation, the temperature distribution of solid region is calculated by FVM and the flow in nozzle is solved by DSMC method [28]. Information exchanges are conducted as follows:

- (1) The heat flux calculated from the flow field by DSMC method was taken as boundary condition for the nozzle;
- (2) The nozzle wall temperature solved by energy equation was set as input for DSMC simulation of nozzle of nozzle flow;
- (3) Such procedure was repeated until converged solution was reached.

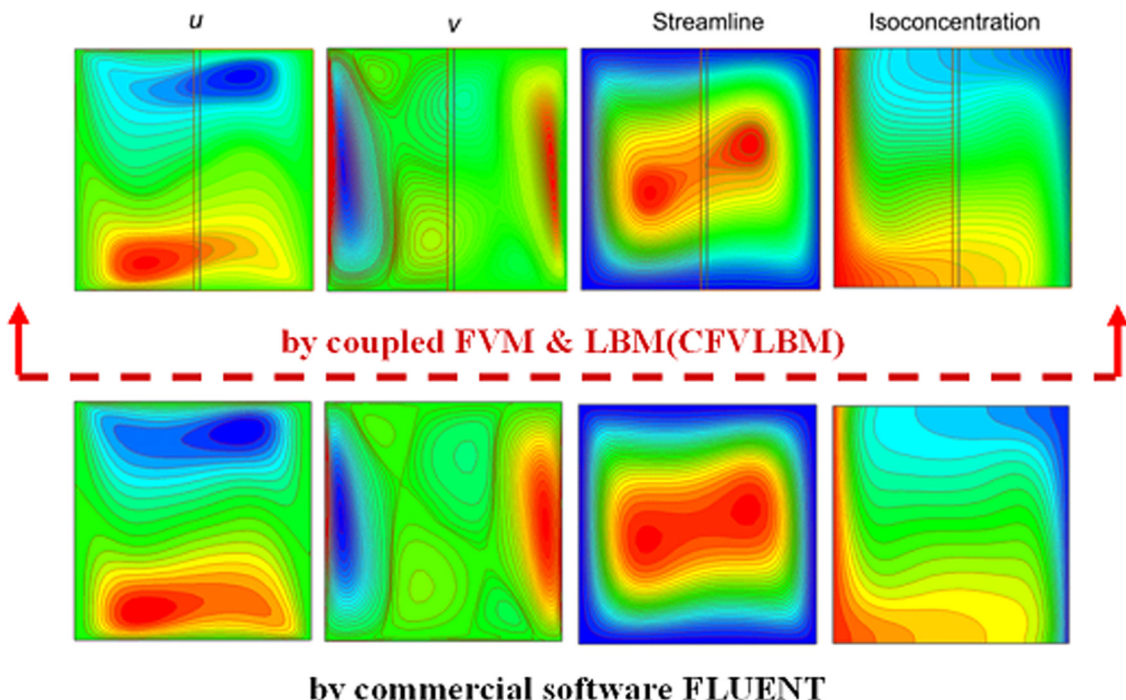


Fig. 12 Comparison of simulation results for natural convection in a square cavity caused by concentration gradient [23]

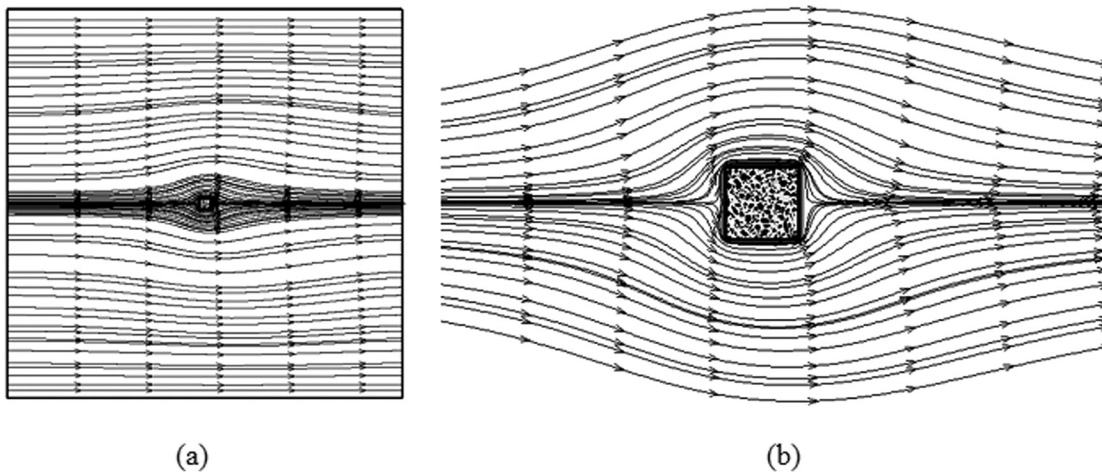


Fig. 13 Flow around a porous square cylinder [29]. (a) Flow around a square cylinder and (b) details of flow field.

3 Numerical Examples Solved by Coupled Multiscale Approach

In this section, four coupled multiscale examples are provided based on the above-mentioned numerical methods.

3.1 Natural Convection in a Square Cavity Caused by Concentration Gradient. The physical problem is shown in Fig. 11. The given conditions are: Sc ($Sc = \nu/D$) = 0.71, $\rho = 1.0 \text{ kg m}^{-3}$, and $\nu = 1.3 \times 10^{-5} \text{ m}^2 \text{ s}^{-1}$. The FVM and LBM are adopted in the left and right parts, respectively, with the center

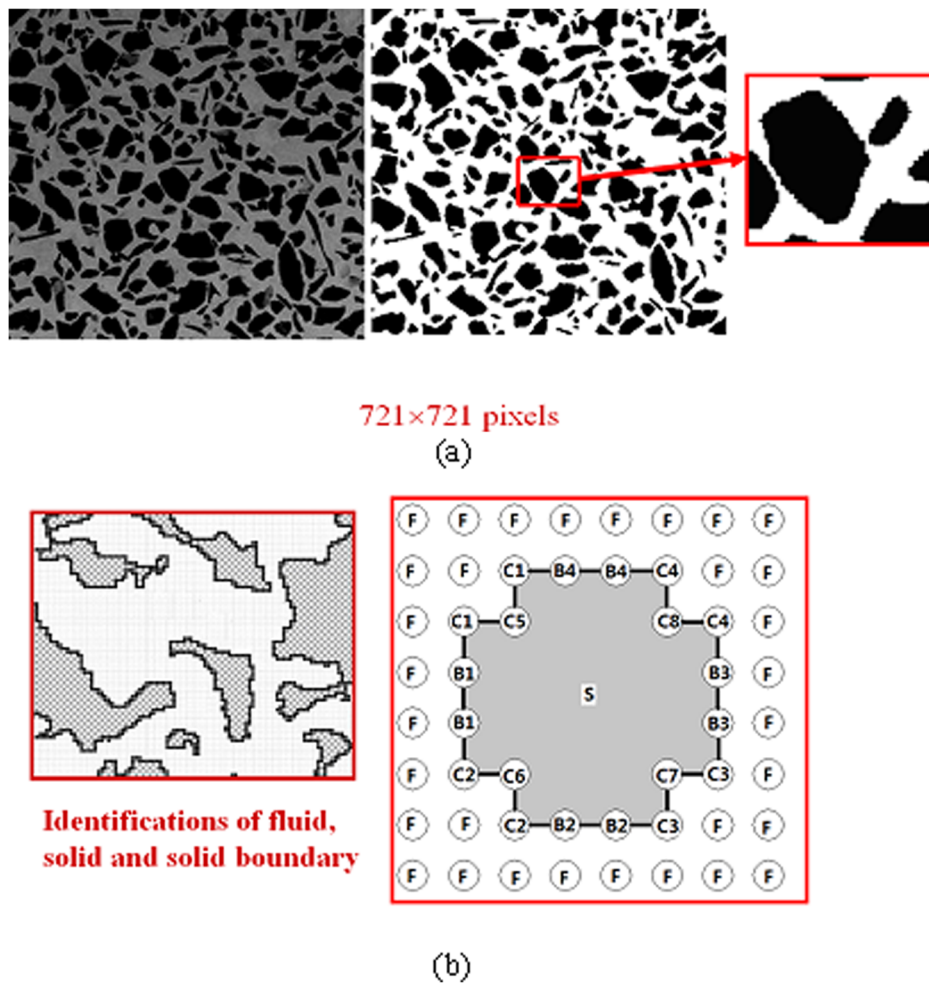


Fig. 14 Treatment of irregular region by LBM [29]. (a) Resolution of porous medium region and (b) detail of treatment of irregular solid region.

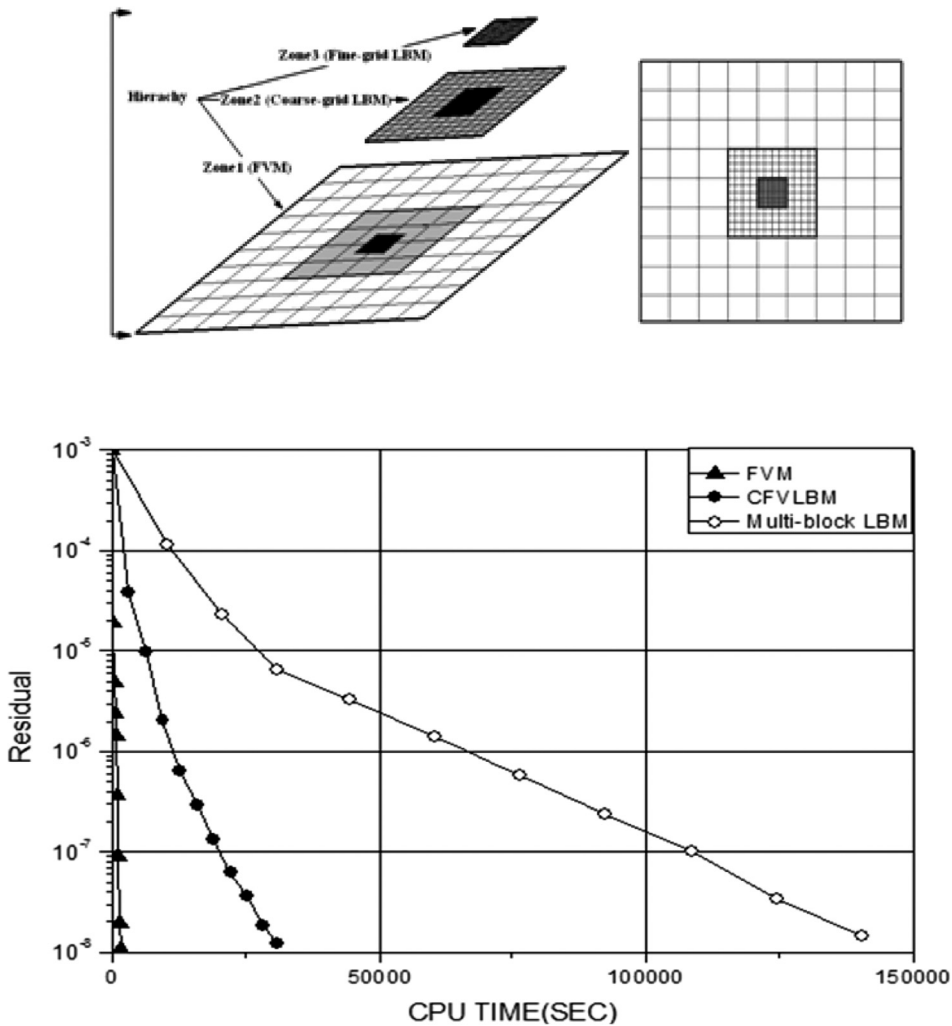


Fig. 15 In the figure the FVM symbols represent the solution procedure for flow around a solid (rather than porous) square cylinder

vertical block as the HR. Simulated results for velocity, streamlines and concentration are compared with those from FLUENT (Fig. 12), and good agreement is reached, showing the feasibility of the coupled method [23].

3.2 Flow Around/Through a Porous Square Cylinder. As shown in Fig. 13(a), a fluid flows through/around a square porous media cylinder [29]. It is obvious that the porous media zone needs high resolution and the other zone may be much coarser. LBM is adopted for the region closely around the cylinder and the region is simulated by FVM with a grid space ratio of 5. The square cylinder is divided into 281 grids \times 281 grids. Figure 13(b) shows more flow information in the porous region. In Fig. 14(a) the resolution of the porous region is shown, and the treatment of irregular solid region is presented in Fig. 14(b). The LBM results can give more detailed flow information within the porous region with the adopted resolution, for interested readers Ref. [29] can be referred. It can be seen that without such coupled numerical method it would be very difficult to resolve such complex flow field by FVM with a reasonable computational time consumption (see Fig. 15). In the figure the FVM symbols represent the solution procedure for flow around a solid (rather than porous) square cylinder.

3.3 Transport Processes in a Mini-PEMFC. A mini-PEMFC model is presented in Fig. 16, where the unit of dimension is mm. In the computation, the diffusion and catalyst layer

are simulated by LBM and the flow channel is predicted by FVM. The results of flow field are presented in Fig. 17. Figure 17(a) shows that due to the blockage of the solid rectangles in the gas diffusion layer (GDL), air mainly flows in the gas channel (GC) and magnitude of velocity in the GC is significantly greater than

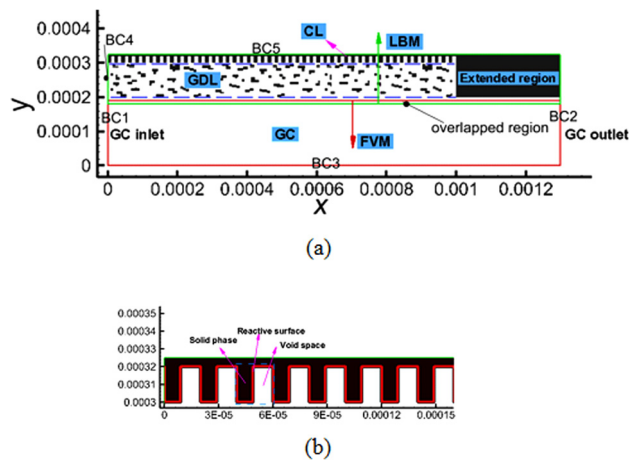


Fig. 16 A mini-PEMFC model. (a) Computational domain and (b) simplified model of catalyst layer.

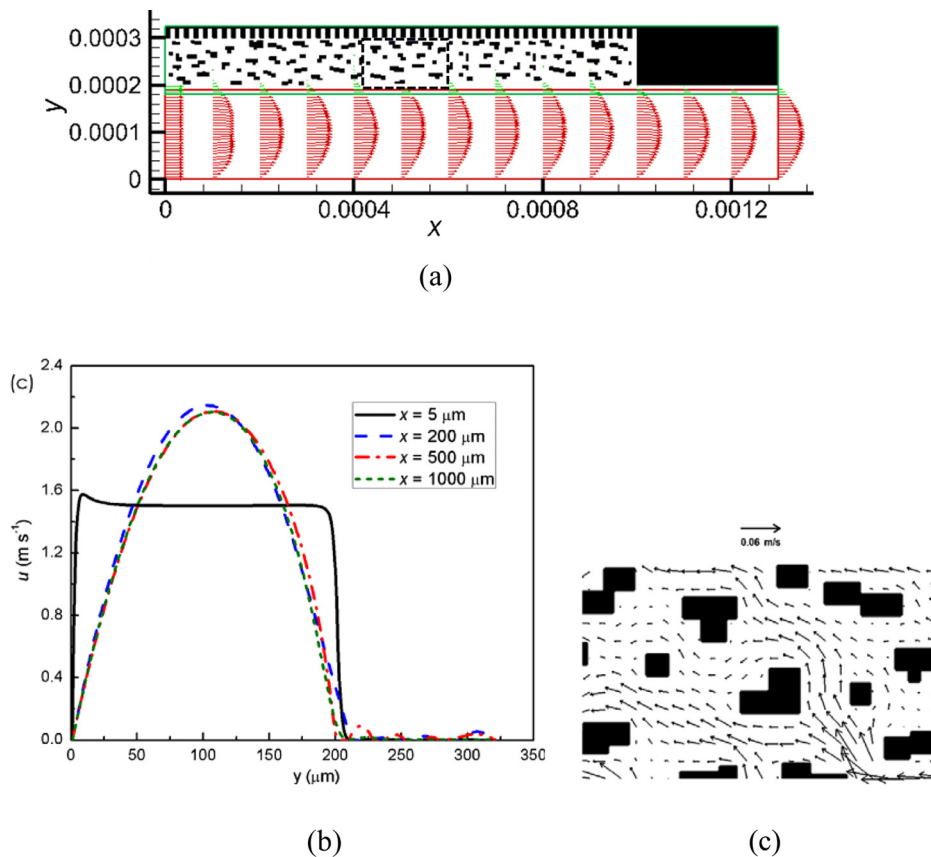


Fig. 17 Coupled simulation results of flow field [22]. (a) Velocity distribution along x-direction, (b) details of u -velocity at four stations, and (c) details of local flow field.

that in the GDL. Figure 17(b) further shows the velocity distribution along the flow direction (x direction). It can be seen that velocity profile shows a parabolic shape in the GC and velocity in GDL is extremely low. Figure 17(c) displays the local detailed velocity vectors in the dashed rectangle shown in Fig. 17(a). It can be seen that fluid flow in the GDL is very complicated due to the complex porous structures of the GDL [22].

It is worth mentioning that even though the computational domain is very small; however, the scientific significance of such a simulation is valuable. Because the flow and mass transport empirical relations in the GDL including empirical relations for permeability and effective diffusivity, which are widely used in macroscopic

simulations based on continuum models of PEMFC, are completely discarded in our simulation, and this is the original significance of the multiscale simulation for a PEMFC as mentioned in Sec. 1.

3.4 Flow Around a Carbon Nanotube (CNT) (MDS–LBM Coupling). The flow of liquid argon around a CNT (Fig. 18) is investigated using the MDS–LBM coupled method. All the configuration parameters are the same as Refs. [31] and [32]. The CNT is located at the center of the whole computational domain. Simulation results by coupled MDS–LBM are compared with the results of pure MDS in Fig. 19 [30], and the agreement is very

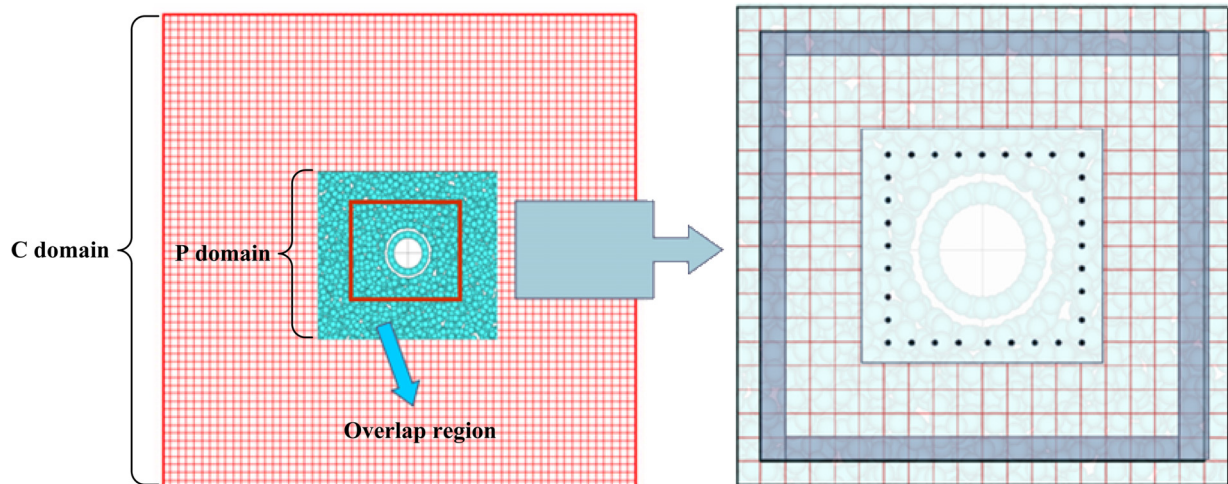


Fig. 18 Flow past a nanotube

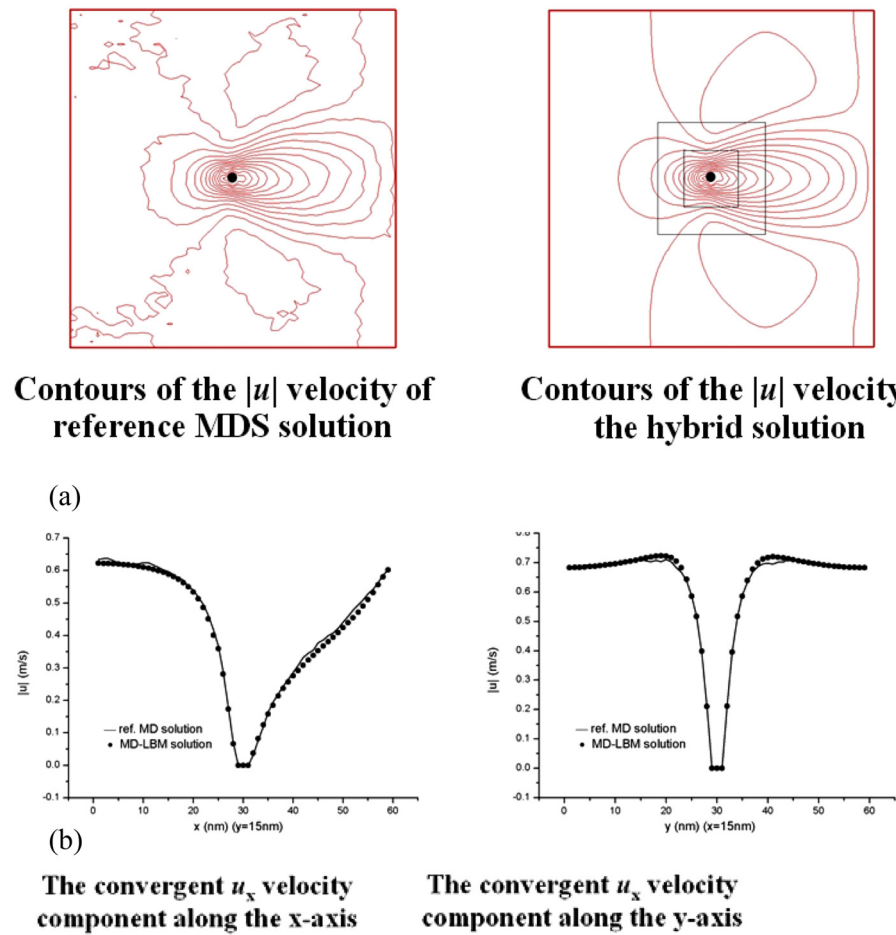


Fig. 19 Comparisons of numerical results by pure MDS and coupled MDS-LBM [30]. (a) Comparison of contours of absolute value of u and (b) comparison of velocity components.

good, with the streamlines from coupled method being much smoother than that of pure MDS. However, as far as the computational time is concerned, the time consumption of the coupled scheme is only about one-fifth of that of the pure MDS simulation.

More coupled example between MDS and FVM can be found in Ref. [33].

Finally, it is worth noting that in this paper for the macroscale methods FDM/FVM/FEM are mentioned as representative methods. Recently quite a few meshfree particle methods, such as smoothed particle hydrodynamics (SPH), have been proposed and applied in heat transfer and fluid flow problems. Even though these methods are termed as particle methods, they are actually macroscale in nature. For some cases, coupling between the solutions of, say, SPH and MDS may be needed. Interesting readers may refer to Refs. [35–37].

4 Further Research Needs

A perfect example of coupled multiscale simulation in material science is presented by Abraham in 2000 [34]. For investigating the propagation of a microcrack at the very sensitive sharp corner of the crack the coupled quantum tight-binding and MDS is used, far from the crack FEM is adopted and around the microcrack MDS is used; then at the interface MDS and FEM are coupled. For the PEMFC, such fully multiscale simulation may be performed as shown in Fig. 20.

With the present day computer resource and numerical algorithms, such fully multiscale simulation for PEMFC is not possible mainly because the needs of huge memory and computational time of MDS of the transport process through the membrane and the simulation of the catalyst chemical reaction at nano/micro-scale level. New and advanced numerical simulation methods are highly required. To the best of the authors' knowledge, the processes involved in PEMFC are a very typical multiscale heat transfer and fluid flow problem, taking this multiscale problem as an example and considering the numerical approaches in the

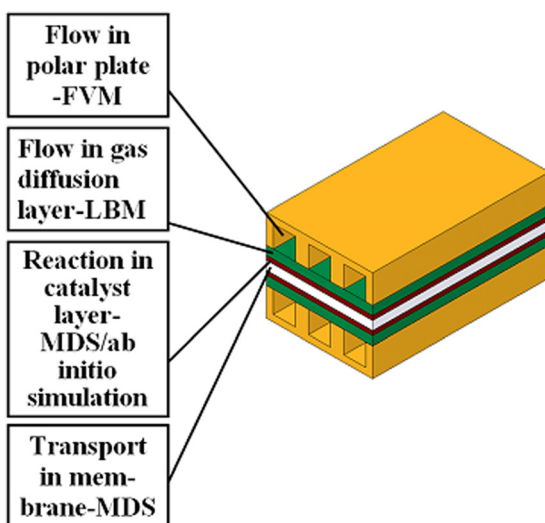


Fig. 20 Fully coupled multiscale simulation of a PEMFC

aforementioned four applications, following further researches are highly required:

- (1) Improve greatly the computational efficiencies of meso-scale and microscale numerical approaches.
- (2) Develop appropriate potential functions for fluids with complex molecule structures (such as water).
- (3) Innovate more efficient coupling techniques for MDS-FVM (MDS-FEM), MDS-LBM, SPH-MDS with high efficiency and stability.
- (4) Develop some upscale model, such as coarse grained (CG)-MDS, for the simulation of transport process through the PEMFC membran.;
- (5) Develop an appropriate coupling model (from ab initio simulation, MDS to some mesoscale method) for the reaction process in the catalyst layer.
- (6) Establish uncertainty analysis approach for numerical results of multiscale simulations.

Finally, the purpose of multiscale simulation is to appropriately combine macroscale and micro/nanoscale method to reveal physical mechanism in depth and to provide guidance for engineering design which can not be obtained from single scale simulation. This important goal should be always kept in mind by all multiscale simulation researchers.

Acknowledgment

Supports from the following national funds are greatly appreciated:

- (1) Key Project of NNSFC (51136004);
- (2) National Key Basic Research Program of China (973 Program) (2013CB228304).

Thanks are also given to the following authors' students: C. H. Min, J. Sun, H. Xu, H. B. Luan, Z. X. Sun, L. Chen, and W. J. Zhou for their hard work in executing the above research programs.

Nomenclature

- a_T = thermal diffusivity
- C = compression operator
- c_i = lattice speed
- c_s = lattice speed of sound
- D = diffusivity
- f_i = density distribution function of velocity
- f_i^{eq} = equilibrium density distribution function of velocity
- F_b = boundary force
- g_i = density distribution function of temperature or concentration
- g_i^{eq} = equilibrium density distribution function of temperature or concentration
- H = height
- k_B = Boltzmann constant
- Kn = Knudsen number
- m = mass of molecule
- p = pressure
- r_w = distance between atom and boundary
- \mathbf{R} = reconstruction operator
- Ra = Rayleigh number
- S = source term
- Sc = Schmidt number
- T = temperature
- u, v = velocity components
- \mathbf{u} = velocity vector
- Y = concentration

Greek Symbols

- α, β = coordinates in LBM
- $\delta t, \Delta t$ = time step

$\Delta x, \Delta z$	= length step
∇	= gradient
ε	= expansion parameter
ϕ	= micro/mesoscale variable
Φ	= macroscopic variable
ν	= kinematic viscosity
ρ	= density
σ	= characteristic length in L-J potential function
τ	= relaxation factor of density distribution function
τ_g	= relaxation factor of temperature/concentration distribution function
ω_i	= weighting factor
∂_{x_α}	= partial derivative with respect to x_α

Abbreviations

CFVLBM	= coupled FVM and LBM
CG	= coarse grained
CNT	= carbon nanotube
CR	= coupled region
DSMC	= direct simulation of Monte Carlo method
FDM	= finite difference method
FEM	= finite element method
FVM	= finite volume method
GC	= gas channel
GDL	= gas diffusion layer
HR	= hybrid region
LBM	= lattice Boltzmann method
MDS	= molecular dynamic simulation
PEMFC	= proton exchange membrane fuel cell
PR	= particle region
SPH	= smoothed particle hydrodynamics

References

- [1] He, Y. L., and Tao, W. Q., 2012, "Multiscale Simulations of Heat Transfer and Fluid Flow Problems," *ASME J. Heat Transfer*, **134**(3), p. 031018.
- [2] Bernardi, D. M., 1990, "Water-Balance Calculations for Solid Polymer-Electrolyte Fuel Cell," *J. Electrochem. Soc.*, **137**(8), pp. 3344–3350.
- [3] Lum, K. W., and McGuirk, J. J., 2005, "Three-Dimensional Model of a Complete Polymer Electrolyte Membrane Fuel Cell—Model Formulation, Validation and Parametric Studies," *J. Power Sources*, **143**(1–2), pp. 103–124.
- [4] Mazumder, S., and Cole, J. V., 2003, "Rigorous 3-D Mathematical Modeling of PEM Fuel Cells. I. Model Predictions Without Liquid Water Transport," *J. Electrochim. Soc.*, **150**(11), pp. A1503–A1509.
- [5] Um, S., and Wang, C. Y., 2004, "Three-Dimensional Analysis of Transport and Electrochemical Reactions in Polymer Electrolyte Fuel Cells," *J. Power Sources*, **125**(1), pp. 40–51.
- [6] Berning, T., Lu, D. M., and Djilali, N., 2002, "Three-Dimensional Computational Analysis of Transport Phenomena in a PEM Fuel Cell," *J. Power Source*, **106**(1–2), pp. 284–294.
- [7] Senn, S. M., and Poulikakos, D., 2004, "Polymer Electrolyte Fuel Cells With Porous Materials Fluid Distributors and Comparisons With Traditional Channeled Systems," *ASME J. Heat Transfer*, **126**(6), pp. 410–418.
- [8] Hu, G., Fan, J., Chen, S., Liu, Y., and Cen, K., 2004, "Three-Dimensional Numerical Analysis of Proton Exchange Membrane Fuel Cells (PEMFCs) With Conventional and Interdigitated Flow Fields," *J. Power Sources*, **136**(1), pp. 1–9.
- [9] Hu, M., Gu, A., Wang, M., Zhu, X., and Yu, L., 2004, "Three Dimensional, Two Phase Mathematical Model for PEM Fuel Cell. Part I. Model Development," *Energy Convers. Manage.*, **45**(11–12), pp. 1861–1882.
- [10] Tao, W. Q., Min, C. H., Liu, X. L., He, Y. L., Yin, B. H., and Jiang, W., 2006, "Parameter Sensitivity Examination and Discussion of PEM Fuel Cell Simulation Model Validation: Part I. Current Status of Modeling Research and Model Development," *J. Power Source*, **160**(1), pp. 359–373.
- [11] Min, C. H., He, Y. L., Liu, X. L., Yin, B. H., Jiang, W., and Tao, W. Q., 2006, "Parameter Sensitivity Examination and Discussion of PEM Fuel Cell Simulation Model Validation. Part II: Results of Sensitivity Analysis and Validation of the Model," *J. Power Source*, **160**(1), pp. 374–385.
- [12] Tao, W. Q., and He, Y. L., 2009, "Recent Advances in Multiscale Simulation of Heat Transfer and Fluid Flow Problems," *Prog. Comput. Fluid Dyn.*, **9**(3/4/5), pp. 151–157.
- [13] Nie, Q., and Joshi, Y., 2008, "Multiscale Thermal Modeling Methodology for Thermoelectrically Cooled Electronic Cabinets," *Numer. Heat Transfer, Part A*, **53**(3), pp. 225–248.
- [14] Wei, C., Liu, Z.-J., Li, Z.-Y., Qu, Z.-G., He, Y.-L., and Tao, W.-Q., 2014, "Numerical Study on Some Improvements in Passive Cooling System of a Radio Base Station by Multiscale Thermal Modeling Methodology—Part I:

- Confirmation of Simplified Models," *Numer. Heat Transfer, Part A*, **65**(9), pp. 844–862.
- [15] Wei, C., Liu, Z.-J., Li, Z.-Y., Qu, Z.-G., He, Y.-L., and Tao, W.-Q., 2014, "Numerical Study on Some Improvements in Passive Cooling System of a Radio Base Station Base on Multiscale Thermal Modeling Methodology—Part II—Results of Multiscale Numerical Simulation and Subsequent Improvements of Cooling Techniques," *Numer. Heat Transfer, Part A*, **65**(9), pp. 863–884.
- [16] Becker, J., Wieser, C., Fell, S., and Steiner, K., 2011, "A Multi-Scale Approach to Material Modeling of Fuel Cell Diffusion Media," *Int. J. Heat Mass Transfer*, **54**(7–8), pp. 1360–1368.
- [17] Franco, A. A., Coulona, R., de Moraiza, R. F., Cheaha, S.-K., Kachmara, A., and Gabriela, M. A., 2009, "Multiscale Modeling Prediction of PEMFC MEA Durability Under Automotive-Operating Conditions," *ECS Trans.*, **25**(1), pp. 65–79.
- [18] de Moraiza, R. F., Sautetb, P., Loffredab, D., and Francoa, A. A., 2011, "A Multiscale Theoretical Methodology for the Calculation of Electrochemical Observables From Ab Initio Data: Application to the Oxygen Reduction Reaction in a Pt(1 1 1)-Based Polymer Electrolyte Membrane Fuel Cell," *Electrochim. Acta*, **56**(28), pp. 10842–10856.
- [19] O'Connel, S. T., and Thompson, P. A., 1995, "Molecular Dynamics–Continuum Hybrid Computations: A Tool for Studying Complex Fluid Flows," *Phys. Rev. E*, **52**(6), R5792–R5795.
- [20] Xu, H., Luan, H., He, Y. L., and Tao, W.-Q., 2012, "A Lifting Relation From Macroscopic Variables to Mesoscopic Variables in Lattice Boltzmann Method: Derivation, Numerical Assessments and Coupling Computations Validation," *Comput. Fluids*, **54**(1), pp. 92–104.
- [21] Luan, H., Xu, H., Chen, L., and Tao, W.-Q., 2010, "Coupling Between FVM and LBM for Heat Transfer and Fluid Flow," *Chin. Sci. Bull.*, **55**(32), pp. 3128–3140 (in Chinese).
- [22] Chen, L., Luan, H., Feng, Y., He, Y. L., and Tao, W.-Q., 2012, "Coupling Between Finite Volume Method and Lattice Boltzmann Method and Its Application to Fluid Flow and Mass Transport in Proton Exchange Membrane Fuel Cell," *Int. J. Heat Mass Transfer*, **55**(13–14), pp. 3834–3848.
- [23] Chen, L., He, Y.-L., Kang, Q., and Tao, W.-Q., 2013, "Coupled Numerical Approach Combining Finite Volume and Lattice Boltzmann Methods for Multi-scale Multi-Physicochemical Processes," *J. Comput. Phys.*, **255**(1), pp. 83–105.
- [24] Liu, J., Chen, S. Y., Nie, X. B., and Robbins, M. O., 2007, "A Continuum–Atomistic Simulation of Heat Transfer in Micro- and Nano-Flows," *J. Comput. Phys.*, **227**(1), pp. 279–291.
- [25] Sun, J., He, Y. L., and Tao, W. Q., 2009, "Molecular Dynamics–Continuum Hybrid Simulation for Condensation of Gas Flow in a Microchannel," *Microfluid. Nanofluid.*, **7**(3), pp. 407–422.
- [26] Yi, P., Poulikakos, D., Walther, J., and Yadigaroglu, G., 2002, "Molecular Dynamics Simulation of Vaporization of an Ultra-Thin Liquid Argon Layer on a Surface," *Int. J. Heat Mass Transfer*, **45**(10), pp. 2087–2100.
- [27] Zhou, W. J., Luan, H. B., He, Y. L., Sun, J., and Tao, W. Q., 2014, "A Study on Boundary Force Model Used in Multiscale Simulations With Non-Periodic Boundary Condition," *Microfluid. Nanofluid.*, **16**(3), pp. 587–595.
- [28] Sun, Z., Li, Z., He, Y.-L., and Tao, W.-Q., 2009, "Coupled Solid (FVM)–Fluid (DSMC) Simulation of Micro-Nozzle With Unstructured-Grid," *Microfluid. Nanofluid.*, **7**(5), pp. 621–631.
- [29] Luan, H.-B., Xu, H., Chen, L., Sun, D.-L., He, Y.-L., and Tao, W.-Q., 2011, "Evaluation of the Coupling Scheme of FVM and LBM for Fluid Flows Around Complex Geometries," *Int. J. Heat Mass Transfer*, **54**(9–10), pp. 1975–1985.
- [30] Zhou, W. J., Luan, H. B., Sun, J., He, Y. L., and Tao, W. Q., 2012, "A Molecular Dynamics and Lattice Boltzmann Multiscale Simulation for Dense Fluid Flows," *Numer. Heat Transfer, Part B*, **61**(5), pp. 369–386.
- [31] Werder, T., Walther, J. H., and Koumoutsakos, P., 2005, "Hybrid Atomistic–Continuum Method for the Simulation of Dense Fluid Flows," *J. Comput. Phys.*, **205**(1), pp. 373–390.
- [32] Dupuis, A., Kotsalis, E. M., and Koumoutsakos, P., 2007, "Coupling Lattice Boltzmann and Molecular Dynamics Models for Dense Fluids," *Phys. Rev. E*, **75**(4), p. 046704.
- [33] Sun, J., He, Y.-L., Tao, W.-Q., Yin, X., and Wang, H. S., 2012, "Roughness Effect on Flow and Thermal Boundaries in Microchannel/Nanochannel Flow Using Molecular Dynamics–Continuum Hybrid Simulation," *Int. J. Numer. Methods Eng.*, **89**(1), pp. 2–19.
- [34] Abraham, F. F., 2000, "Dynamically Spanning the Length Scales From the Quantum to the Continuum," *Int. J. Mod. Phys. C*, **11**(6), pp. 1135–1148.
- [35] Ganzenmüller, G. C., Hiermaier, S., and Steinhauser, M. O., 2012, "Consistent Temperature Coupling With Thermal Fluctuation of Smooth Particle Hydrodynamics and Molecular Dynamics," *Plos ONE*, **7**(12), p. e51989.
- [36] Liu, B. O., Liu, J., Lu, W. Q., and Ni, M. J., 2012, "Simulation of Liquid Argon Flow in Micro-Channel by an SPH–MD Coupling Method," *J. Eng. Phys.*, **33**(6), pp. 993–996 (in Chinese).
- [37] Xiao, Y., Yuan, J., and Sundén, B., 2012, "Modeling of Micro/Meso-Scale Reactive Transport Phenomena in Catalyst Layers of Proton Exchange Membrane Fuel Cells," *Int. J. Low Carbon Technol.*, **7**(4), pp. 280–287.